

Impact of the Fe Doping on Magnetism in Perovskite Cobaltites

Xigang Luo, Wendong Xing, Zhaofeng Li, Gang Wu, and Xianhui Chen*

*Hefei National Laboratory for Physical Science at Microscale and Department of Physics,
University of Science and Technology of China,
Hefei, Anhui 230026, People's Republic of China*

Abstract

We systematically studied the magnetic and transport properties for the polycrystalline samples of Fe-doped perovskite cobaltites: $\text{Pr}_{1-y}\text{Ca}_y\text{Co}_{1-x}\text{Fe}_x\text{O}_3$ ($y=0.3$, $x=0-0.15$; $y=0.45$, $x=0-0.3$) and $\text{Gd}_{0.55}\text{Sr}_{0.45}\text{Co}_{1-x}\text{Fe}_x\text{O}_3$ ($x=0-0.3$). Fe doping leads to an enhancement of the ferromagnetism in the systems of $\text{Pr}_{1-y}\text{Ca}_y\text{Co}_{1-x}\text{Fe}_x\text{O}_3$, while the ferromagnetism is suppressed with further increasing Fe content and spin-glass behavior is observed at high doping level of Fe. In contrast, the ferromagnetism is suppressed in the system $\text{Gd}_{0.55}\text{Sr}_{0.45}\text{Co}_{1-x}\text{Fe}_x\text{O}_3$ as long as Fe is doped, and no spin-glass behavior is observed in the sample with Fe doping up to 0.3. The competition between ferromagnetic interactions through $\text{Fe}^{3+}\text{-O-(LS)Co}^{4+}$ and antiferromagnetic interactions through $\text{Fe}^{3+}\text{-O-Fe}^{3+}$ and $\text{Fe}^{3+}\text{-O-(IS)Co}^{3+}$ is considered to be responsible for the behavior observed above. The average radius of the ions on A sites plays the key role in determining what type of interactions Fe doping mainly introduces.

PACS numbers: 75.47.Pq, 75.30.-m, 75.30.Et, 75.50.Lk

I. INTRODUCTION

Transition-metal oxides with perovskite-type crystal structure attracted a great deal of interests in the past two decades due to the fascinating characters of superconducting, magnetic and transport properties. These properties range from high-temperature superconductivity,[1] colossal magnetoresistance,[2] ferroelectricity,[3, 4] multiferroics,[5, 6, 7] to co-incident metal-insulator, structural, and magnetic phase transitions.[8] The perovskite cobaltites ACoO_3 was discovered in 1950s[9, 10]. But they still attracted interests due to a couple of unique properties; namely, the large magnetoresistance (MR),[11] enormous Hall effect,[12, 13] the existence of the spin-state transitions,[8, 14, 15, 16, 17] and the unusual magnetic ground states of doped cobaltites.[19, 20, 21, 22]

The distinct feature in perovskite cobaltites compared to other transition-metal oxides such as manganites is the existence of various spin states of Co ions. Recent experimental and theoretical investigations on perovskite cobaltites indicate that the spin states are low-spin (LS) and the mixture of intermediate-spin(IS)/LS for tetravalent and trivalent cobalt ions, respectively.[23, 24, 25, 26, 27, 28, 29] This behavior arises from the fact that the crystal field splitting of Co d states (Δ_{CF}) and the Hund's rule exchange energy (J_{H}) are comparable in magnitude for the cobaltites, which means that the energy gap ($\delta E = \Delta_{\text{CF}} - J_{\text{H}}$) between t_{2g} and e_g bands is rather small. In fact, this gap can be of the order of 10 meV in LaCoO_3 , so that the electrons in t_{2g} levels can be thermally excited to the e_g states, leading to higher spin states of Co ions.[8] Because Δ_{CF} is very sensitive to the variation in the Co-O bond length ($d_{\text{Co-O}}$) or the unit cell volume of lattice, the subtle balance between Δ_{CF} and J_{ex} may be easily disrupted by different kinds of effect, such as the hole-doping and the chemical/external pressure.[30, 31, 32, 33] The "intermediate spin state" has been claimed to exist in $\text{La}_{1-x}\text{Sr}_x\text{CoO}_3$ by different groups.[18, 19, 24, 29] It is generally accepted that the ferromagnetism in hole-doped $\text{La}_{1-x}\text{M}_x\text{CoO}_3$ ($\text{M} = \text{Ca}, \text{Sr}, \text{and Ba}$) results from the double-exchange (DE) interaction between Co^{3+} and Co^{4+} ions, facilitating also the electrical conductivity in the ferromagnetic metallic phase. In this consideration, the DE interaction is accomplished through transfer of e_g electrons in the intermediate-spin (IS) Co^{3+} to LS Co^{4+} , so that the e_g electrons become collective in $\text{La}_{1-x}\text{Sr}_x\text{CoO}_3$ and the Co ions ultimately turn into $t_{2g}^5 e_g^x$ electronic configuration. For the cobaltites (such as: $\text{Pr}_{1-y}\text{Ca}_y\text{CoO}_3$ and $\text{Nd}_{1-y}\text{Ca}_y\text{CoO}_3$) with small average radius of ions on A sites, resistivity

is not metallic in these compounds, meaning that the magnetic exchange should be localized to some extent instead of being itinerant as in DE exchange. Therefore, further studies to make clear the magnetic exchange interactions in cobaltites are desired.

If Co ions are partially substituted by other transition metal ions, the DE interaction between Co^{3+} and Co^{4+} will be destroyed to some extent. In addition, magnetic exchange interactions between Co ions and the doped transition-metal ions could be expected because the existence of various valence and spin-states of Co ions. Investigation on such interactions through substituting Co ions by other transition ions would be expected helpfully to make the role of all kinds of spin-states and valences in the magnetic exchange interactions clear. In the present paper, we choose Fe element as the substitution ion. The effect of Fe doping in $\text{La}_{1-x}\text{Sr}_x\text{CoO}_3$ has been studied by several groups,[34, 35, 36, 37, 38] and the common conclusion is the suppression of ferromagnetism and metallicity with Fe doping as a result of the diluting of ferromagnetic interaction of $\text{Co}^{3+}\text{-O-Co}^{4+}$ and the introduction of the antiferromagnetic exchange interactions Fe-O-Fe and Fe-O-Co. However, Our recent work on $\text{Pr}_{0.5}\text{Ca}_{0.5}\text{Co}_{1-x}\text{Fe}_x\text{O}_{3-\delta}$ gave the evidence that Fe doping enhances the ferromagnetism.[39] The contrasting results observed in $\text{La}_{1-x}\text{Sr}_x\text{CoO}_3$ and $\text{Pr}_{0.5}\text{Ca}_{0.5}\text{CoO}_{3-\delta}$ with Fe doping could give some constructive hints on the magnetic interactions and spin states in the two systems. Because the existence of spin-state transition with temperature in $\text{Pr}_{0.5}\text{Ca}_{0.5}\text{CoO}_{3-\delta}$, [17, 39] it is not suitable to be used for investigating the magnetic interactions between Co and Fe ions. Therefore, we choose two systems with less Ca content, which do not exhibit spin-state transition at low temperature.[40] As a comparison, the system $\text{Gd}_{0.55}\text{Sr}_{0.45}\text{CoO}_3$, which has the similar magnetic and transport properties to the typical $\text{La}_{1-x}\text{Sr}_x\text{CoO}_3$, [41] was chosen as another object for Fe doping. The distinct responses of magnetic properties to the Fe doping are observed due to the different average ionic radius of A site.

II. EXPERIMENTAL DETAILS

Polycrystalline $\text{Pr}_{1-y}\text{Ca}_y\text{Co}_{1-x}\text{Fe}_x\text{O}_3$ ($y=0.3, x=0-0.15; y=0.45, x=0-0.3$) and $\text{Gd}_{0.55}\text{Sr}_{0.45}\text{Co}_{1-x}\text{Fe}_x\text{O}_3$ ($x=0-0.3$) samples were prepared through the conventional solid-state reaction. For $\text{Pr}_{0.7}\text{Ca}_{0.3}\text{Co}_{1-x}\text{Fe}_x\text{O}_3$ and $\text{Pr}_{0.55}\text{Ca}_{0.45}\text{Co}_{1-x}\text{Fe}_x\text{O}_3$ samples, the powders of Pr_6O_{11} , CaCO_3 , Co_3O_4 , and Fe_2O_3 were mixed in stoichiometric proportion and heated

at 1200 °C in the flowing oxygen for 24 h. The mixture was ground and pressed into pellets and finally sintered at 1200 °C in flowing oxygen for 24 h twice. $\text{Gd}_{0.55}\text{Sr}_{0.45}\text{Co}_{1-x}\text{Fe}_x\text{O}_3$ samples were fabricated from the stoichiometric amount of Gd_2O_3 , SrCO_3 , and Co_3O_4 and Fe_2O_3 powders. The mixtures were fired at 1200 °C for 24 h in air, then reground and pressed into pellets which were sequently sintered at 1200 °C for 24 h. This procedure was then repeated two times. Because in these as-fabricated cobaltites a large amount of oxygen vacancies exist,[39, 41] the samples need to be post-annealed under high pressure oxygen to achieve oxygen stoichiometry. $\text{Pr}_{1-y}\text{Ca}_y\text{Co}_{1-x}\text{Fe}_x\text{O}_3$ samples were then annealed at 600 °C under the high oxygen pressure of 265 atm for 48 h. The $\text{Gd}_{0.55}\text{Sr}_{0.45}\text{Co}_{1-x}\text{Fe}_x\text{O}_3$ samples were annealed at 900 °C under the high oxygen pressure of 260 atm for 24 h.

X-ray diffraction (XRD) data were collected using $\text{Cu } K_\alpha$ radiation ($\lambda = 1.5418\text{\AA}$) at room temperature. Direct and alternating current (dc and ac) magnetic measurements were performed with a superconducting quantum interference device (SQUID) magnetometer (MPMS-7XL, Quantum Design). Resistivity was measured by using the standard ac four-probe method. The oxygen content of the samples were determined by using the $\text{K}_2\text{Cr}_2\text{O}_7$ titration method.[39, 41] The results indicated that after annealing under the high pressure oxygen the oxygen vacancies are controlled less than 0.01 for the $\text{Gd}_{0.55}\text{Sr}_{0.45}\text{Co}_{1-x}\text{Fe}_x\text{O}_3$ samples and 0.005 for the $\text{Pr}_{1-y}\text{Ca}_y\text{Co}_{1-x}\text{Fe}_x\text{O}_3$ samples.

III. EXPERIMENTAL RESULTS

A. Structural Characterization

XRD patterns indicated that all the samples are single phase with the orthorhombic structural symmetry (Space Group: Pnma), consistent with our previous reports.[39, 41] The unit cell volumes with Fe concentration are plotted in Fig.1 for the three systems. It indicated that for all the three systems, Fe-doping enlarges the crystal lattice obviously. As one knows, the radius of LS Co^{4+} , LS Co^{3+} , IS Co^{3+} , and high-spin (HS) Co^{3+} is 0.53, 0.545, 0.56 and 0.61 Å, respectively; while the radius of LS Fe^{3+} , HS Fe^{3+} and Fe^{4+} is 0.55, 0.645 and 0.585 Å, respectively.[42] Consequently, the rapid enlargement of unit cell volume shown in Fig. 1 strongly suggested that the doped Fe ions is Fe^{3+} ions with a high-spin (HS) $t_{2g}^3 e_g^2$ electronic configuration, consistent with the results obtained by the Mössbauer experiments

in the other Fe-doped perovskite cobaltites $\text{TbBaCo}_2\text{O}_{5.5}$ and $\text{La}_{1-x}\text{Sr}_x\text{CoO}_3$. [37, 43, 44]

B. Magnetic properties

Temperature dependence of zero-field cooled (ZFC) and field-cooled (FC) molar magnetization ($H = 0.1$ T) is shown in Fig. 2 for $\text{Gd}_{0.55}\text{Sr}_{0.45}\text{Co}_{1-x}\text{Fe}_x\text{O}_3$ samples. Fig. 2 shows that the ferromagnetism is suppressed as any Co ions are substituted by Fe ions. The Fe-free sample has $T_c \approx 125$ K (T_c is determined from the maximum of the FC $dM(T)/dT$), while for the sample with $x = 0.30$, T_c decreases to about 95 K. The magnetization at 4 K is also reduced from 10500 emu/mol for $x = 0$ to 3000 emu/mol for $x = 0.3$ except for the enhancement for $x = 0.1$. The effect of Fe doping in $\text{Gd}_{0.55}\text{Sr}_{0.45}\text{CoO}_3$ seems to be the same as that in $\text{La}_{1-x}\text{Sr}_x\text{CoO}_3$. [35, 36] In $\text{La}_{1-x}\text{Sr}_x\text{CoO}_3$, ferromagnetism are suppressed when Co ions are substituted by Fe ions, and spin-glass behavior is induced with further increasing Fe concentration. [36] However, no spin-glass behavior can be observed in $\text{Gd}_{0.55}\text{Sr}_{0.45}\text{Co}_{1-x}\text{Fe}_x\text{O}_3$ even with x up to 0.3. It is confirmed from the ac susceptibility measurements. Temperature dependence of in-phase ac susceptibility ($\chi'(T)$) is shown in Fig. 3 for three samples with $x = 0, 0.15$ and 0.3 . $\chi'(T)$ is measured in an ac magnetic field of $H = 3.8$ Oe at 1 and 1000 Hz, respectively. Strong peaks can be observed for all the $\chi'(T)$ curves around the temperature where the dM/dT reaches maximum, suggesting that the peaks in the $\chi'(T)$ curves correspond to the ferromagnetic transition. The position of the peak at different frequencies shifts less than 1 K ($\leq 1\%$). Therefore, the frequency independent- $\chi'(T)$ suggests no spin-glass behavior even for the sample with $x=0.30$, consistent with that observed in the $M(T)$ curves. This behavior is in contrast to the case of $\text{La}_{1-x}\text{Sr}_x\text{Co}_{1-x}\text{Fe}_x\text{O}_3$, in which a spin glass state is induced in the sample with large x . [36] The very weak shift of the peak position with frequency could arise from the cluster nature of the ferromagnetism in the perovskite cobaltites. [22]

More intriguing magnetism with Fe doping is observed in $\text{Pr}_{1-y}\text{Ca}_y\text{CoO}_3$ ($y = 0.3$ and 0.45) systems. Figure 4 shows temperature dependence of the ZFC and FC molar magnetization for the $\text{Pr}_{1-y}\text{Ca}_y\text{Co}_{1-x}\text{Fe}_x\text{O}_3$ ($y=0.3, x=0-0.15$; $y=0.45, x=0-0.3$) samples. Ferromagnetic transition occurs at $T_c \approx 69$ K for $y = 0.45$ and 46 K for $y = 0.3$ in the Fe-free samples, respectively. With Fe doping, T_c increases firstly and then decreases for the two series of samples with different y . It suggests that ferromagnetism in the two series of sam-

ples is enhanced firstly, and then suppressed with further increasing Fe concentration. For the highly doped samples $\text{Pr}_{0.55}\text{Ca}_{0.45}\text{Co}_{0.7}\text{Fe}_{0.3}\text{O}_3$ and $\text{Pr}_{0.7}\text{Ca}_{0.3}\text{Co}_{0.85}\text{Fe}_{0.15}\text{O}_3$, spin-glass behavior is observed, being in contrast to the case of $\text{Gd}_{0.55}\text{Sr}_{0.45}\text{Co}_{1-x}\text{Fe}_x\text{O}_3$ samples.

To clarify the magnetic nature of the data in Fig.4, the ZFC $\chi'(T)$ was measured in the magnetic field of $H = 3.8$ Oe at 1 and 1000 Hz for all the samples. The results are shown in Fig.5 and Fig.6, respectively. It is found that the position of the peaks is only 2-3 K different from the temperature of maximum of dM/dT (T_c) for the slightly doped samples, while more than 10 K for the highly doped samples (15 K for $\text{Pr}_{0.55}\text{Ca}_{0.45}\text{Co}_{0.7}\text{Fe}_{0.3}\text{O}_3$ and 11 K for $\text{Pr}_{0.7}\text{Ca}_{0.3}\text{Co}_{0.85}\text{Fe}_{0.15}\text{O}_3$). Frequency dependence of the peak position is almost independent for the slightly doped samples (less than 1 K in Fig.5(a-d) and Fig.6(a-c), while the peak position is strongly frequency-dependent for the samples with $x = 0.3$ for $y = 0.45$ and $x \geq 0.1$ for $y = 0.3$, and the temperature of peaks shifts larger than 5% at two different frequencies of 1 Hz and 1 KHz as shown in Fig.5e and Fig.6e, indicative of the obvious spin-glass behavior. The frequency dependence is a direct indication of the slow spin dynamics, indicating the peaks in Fig.5e and Fig.6e associated with the spin-glass freezing temperature T_f . The frequency dependence is illustrated more clearly in Fig.7, it shows the "closeup" of the peaks in $\chi'(T)$ shown in Fig.5e. It is found that the T_f increases monotonically with increasing frequency f , further confirming the spin-glass state in $\text{Pr}_{0.55}\text{Ca}_{0.45}\text{Co}_{0.7}\text{Fe}_{0.3}\text{O}_3$. The frequency dependence can be well described by the conventional critical "slowing down" of the spin dynamics, [45, 46] as described by

$$\frac{\tau}{\tau_0} \propto \left(\frac{T_f - T_{SG}}{T_{SG}} \right)^{-z\nu} \quad (1)$$

where τ_0 is the characteristic time scale for the spin dynamics(i.e., the relaxation time), $\tau=f^{-1}$, T_{SG} is the critical temperature for spin-glass ordering (this is equivalent to the value of T_f when $f \rightarrow 0$) and $z\nu$ is a constant exponent (in which ν is the critical exponent of the correlation length and z the dynamic exponent). The best fit to the data using the Eq. (1) is obtained by choosing the value of T_{SG} which minimizes the least-square deviation from a straight-line fit (See Fig.8). The values of τ_0 and $z\nu$ are extracted from the intercept and slope, respectively. For $\text{Pr}_{0.55}\text{Ca}_{0.45}\text{Co}_{0.7}\text{Fe}_{0.3}\text{O}_3$, $T_{SG} = 51.81$ K, $z\nu = 6.85$, and $\tau_0 = 1.37 \times 10^{-12}$ s, which is larger than that of conventional spin glasses ($\sim 10^{-13}$ s), indicating a slower spin dynamics. τ_0 is larger than that obtained in $\text{La}_{1-x}\text{Sr}_x\text{CoO}_3$ ($x < 0.18$),[19] but smaller than that achieved in Fe-doped $\text{La}_{0.5}\text{Sr}_{0.5}\text{CoO}_3$. [36]

C. Transport Behaviors

Although the effect of Fe-doping on the magnetism is different for $\text{Gd}_{0.55}\text{Sr}_{0.45}\text{CoO}_3$ and $\text{Pr}_{1-y}\text{Ca}_y\text{CoO}_3$ ($y = 0.3$ and 0.45) systems, the evolution of resistivity with Fe doping shows similar. Temperature dependence of the resistivity for the three series of samples is shown in Fig. 9. The zero field data indicate that the $\text{Gd}_{0.55}\text{Sr}_{0.45}\text{CoO}_3$ is metallic ($d\rho/dT > 0$) in the whole measuring temperature range, while semiconducting behavior ($d\rho/dT < 0$) is observed above T_c for $\text{Pr}_{1-y}\text{Ca}_y\text{CoO}_3$ ($y = 0.3$ and 0.45) samples. The evolution of resistivity with Fe doping is similar among all the three systems: it is found that the resistivity increases monotonically with increasing Fe doping level; the highly Fe-doped samples show an insulating behavior in the whole temperature range. These results are similar to those observed in $\text{La}_{0.5}\text{Sr}_{0.5}\text{Co}_{1-x}\text{Fe}_x\text{O}_3$ samples.[36] Resistivity results suggest that Fe doping leads to strong localized feature, and the conductive channels between Co ions are broken near Fe atoms.

IV. DISCUSSIONS

The transport and magnetization data indicate that the $\text{Gd}_{0.55}\text{Sr}_{0.45}\text{CoO}_3$ has much higher ferromagnetic transition temperature relative to $\text{Pr}_{1-y}\text{Ca}_y\text{CoO}_3$. However, $\text{Gd}_{0.55}\text{Sr}_{0.45}\text{CoO}_3$ has much lower ferromagnetic transition temperature relative to the same Sr doping level in $\text{La}_{1-x}\text{Sr}_x\text{CoO}_3$. [39] The ferromagnetic transition strongly depends on the average radius of ions on A sites ($\langle r_A \rangle$), so that the La-, Pr- and Gd-based systems show different ferromagnetic transition temperature ($\langle r_{\text{La}_{0.55}\text{Sr}_{0.45}} \rangle = 1.258 \text{ \AA}$, $\langle r_{\text{Gd}_{0.55}\text{Sr}_{0.45}} \rangle = 1.198 \text{ \AA}$, $\langle r_{\text{Pr}_{0.55}\text{Ca}_{0.45}} \rangle = 1.179 \text{ \AA}$)[47]. This is because the average radius of ions on A sites ($\langle r_A \rangle$) strongly affects the band width [48], consequently on T_c . In general, band width and T_c decreases with decreasing $\langle r_A \rangle$. The band width directly influences the transport behavior. As shown in Fig.9, the Fe-free $\text{Gd}_{0.55}\text{Sr}_{0.45}\text{CoO}_3$ sample shows metallic behavior in the whole temperature range, similar to that of $\text{La}_{1-x}\text{Sr}_x\text{CoO}_3$. It suggests that holes should be itinerant, so that e_g is considered to be collective. Consequently, most of the Co ions (except for some LS trivalent Co ions) in $\text{Gd}_{0.55}\text{Sr}_{0.45}\text{CoO}_3$ have intermediate $t_{2g}^5 e_g^\delta$ electronic configuration. However, $\text{Pr}_{0.55}\text{Ca}_{0.45}\text{CoO}_3$ shows weakly metallic behavior only above 250 K and becomes insulating below 250 K. The different temperature dependence of resistivity

in $\text{Gd}_{0.55}\text{Sr}_{0.45}\text{CoO}_3$ and $\text{Pr}_{0.55}\text{Ca}_{0.45}\text{CoO}_3$ could be understood with the different $\langle r_A \rangle$. Larger $\langle r_A \rangle$ in $\text{Gd}_{0.55}\text{Sr}_{0.45}\text{CoO}_3$ leads to a larger band width, so that it is metallic below room temperature; while smaller $\langle r_A \rangle$ in $\text{Pr}_{0.55}\text{Ca}_{0.45}\text{CoO}_3$ results in a narrower band width, so that it shows insulating behavior in $T_c < T < 250\text{K}$, indicative of the obvious localized feature.

Mössbauer experiments[37, 43, 44] have demonstrated that the doped Fe ions in the perovskite cobaltites have the formation of Fe^{3+} with a high-spin $t_{2g}^3 e_g^2$ electronic configuration. The rapid enlargement of lattice volume with Fe doping shown in Fig.1 further confirms that the Fe ions have such formation in the present three series of samples. Recent investigations support the configuration of LS Co^{4+} and the mixed IS/LS Co^{3+} in perovskite cobaltites.[23, 24, 25, 26, 27, 28, 29] By fitting the susceptibility above T_c with the Curie-Weiss law after subtracting the contribution of Gd^{3+} ($7.94\mu_B$)/ Pr^{3+} ($3.58\mu_B$) ions, the effective moment per Co ion is obtained as $2.362\mu_B$ and $2.368\mu_B$ for $\text{Gd}_{0.55}\text{Ca}_{0.45}\text{CoO}_3$ and $\text{Pr}_{0.55}\text{Ca}_{0.45}\text{CoO}_3$, respectively. These values are close to that ($2.398\mu_B$) estimated from IS Co^{3+} + LS Co^{4+} configuration for such doping level, indicating that Co^{4+} ions are at LS state and most of the Co^{3+} ions are at IS state in these two compounds. Therefore, the exchange interactions including Fe^{3+} are mainly $\text{Fe}^{3+}\text{-O-Fe}^{3+}$, $\text{Fe}^{3+}\text{-O-Co}^{3+}$ (IS), $\text{Fe}^{3+}\text{-O-Co}^{4+}$ (LS) as shown in Fig.10. According to Goodenough-Kanamori rules, superexchange interactions through $\text{Fe}^{3+}\text{-O-Fe}^{3+}$ are antiferromagnetic, while those through $\text{Fe}^{3+}\text{-O-Co}^{4+}$ (LS) are ferromagnetic.[49, 50, 51] The Goodenough-Kanamori rules can not directly give whether the exchange interactions through $\text{Fe}^{3+}\text{-O-Co}^{3+}$ (IS) are ferromagnetic or antiferromagnetic because the sign of this interaction depends on the relative orientation of the (un-)occupied e_g orbitals. Although the information of the relative orientation of the orbitals in present materials is not available, we could assume an antiferromagnetic exchange interaction through $\text{Fe}^{3+}\text{-O-Co}^{3+}$ (IS) based on the observed results in $\text{Gd}_{0.55}\text{Sr}_{0.45}\text{Co}_{1-x}\text{Fe}_x\text{O}_3$. In $\text{Gd}_{0.55}\text{Sr}_{0.45}\text{CoO}_3$, the exchange interactions through $\text{Fe}^{3+}\text{-O-Co}^{4+}$ (LS) are absent due to the collective feature of the e_g electrons (forming the intermediate $t_{2g}^5 e_g^\delta$ electronic configuration instead of individual LS Co^{4+} and IS Co^{3+} ions). At the low doping level of Fe, Fe ions is diluted so that the interactions through $\text{Fe}^{3+}\text{-O-Co}^{3+}$ (IS) play the main role. Therefore the suppression of the ferromagnetism by slightly doping of Fe suggests that the interactions through $\text{Fe}^{3+}\text{-O-Co}^{3+}$ (IS) should be antiferromagnetic. With increasing Fe concentration, the strong antiferromagnetic exchange interactions through $\text{Fe}^{3+}\text{-O-Fe}^{3+}$ appear and further

suppress the ferromagnetism . In $\text{Pr}_{1-y}\text{Ca}_y\text{CoO}_3$, the e_g electrons have obviously the localized feature as discussed above, so that the Co ions are at LS Co^{4+} and IS Co^{3+} states. For the slightly doping samples, the enhancement of ferromagnetism arises from the ferromagnetic interactions through $\text{Fe}^{3+}\text{-O-Co}^{4+}(\text{LS})$. The enhancement of the ferromagnetism at low Fe doping level suggests that ferromagnetic $\text{Fe}^{3+}\text{-O-Co}^{4+}(\text{LS})$ interaction is stronger than possibly antiferromagnetic $\text{Fe}^{3+}\text{-O-Co}^{3+}(\text{IS})$ one, so that the ferromagnetic $\text{Fe}^{3+}\text{-O-Co}^{4+}(\text{LS})$ interactions are expected to play the main role in the slight Fe-doped samples. However, with further increasing Fe concentration, the interactions through $\text{Fe}^{3+}\text{-O-Fe}^{3+}$ increase dramatically. According to Goodenough-Kanamori rules, the exchange interactions through $\text{Fe}^{3+}\text{-O-Fe}^{3+}$ is stronger than those through $\text{Fe}^{3+}\text{-O-Co}^{4+}(\text{LS})$. [51] In this case, the antiferromagnetic $\text{Fe}^{3+}\text{-O-Fe}^{3+}$ interactions gradually become dominating.

It is well known that the competition between ferromagnetic and antiferromagnetic interactions as well as the randomness of magnetic interactions induces the spin-glass magnetism. The antiferromagnetic interactions (through $\text{Fe}^{3+}\text{-O-Co}^{3+}(\text{IS})$ and $\text{Fe}^{3+}\text{-O-Fe}^{3+}$) introduced by Fe doping coexist with the ferromagnetic interactions between Co ions (as well as $\text{Fe}^{3+}\text{-O-Co}^{4+}(\text{LS})$). At the meantime, the disordered distribution of Fe ions on Co sites leads to the strong randomness of (anti)ferromagnetic interactions in the system, consequently induces the magnetic frustration. The two effects induced by Fe doping induce the spin-glass magnetism with increasing Fe concentration. In $\text{Pr}_{0.55}\text{Ca}_{0.45}\text{Co}_{1-x}\text{Fe}_x\text{O}_3$ and $\text{Pr}_{0.7}\text{Ca}_{0.3}\text{Co}_{1-x}\text{Fe}_x\text{O}_3$, the spin-glass behavior is observed in the highly doped samples. It should be pointed out that spin-glass behavior occurs at lower Fe doping level for $\text{Pr}_{0.7}\text{Ca}_{0.3}\text{Co}_{1-x}\text{Fe}_x\text{O}_3$ than for $\text{Pr}_{0.55}\text{Ca}_{0.45}\text{Co}_{1-x}\text{Fe}_x\text{O}_3$. This should arise from the weaker ferromagnetism in $\text{Pr}_{0.7}\text{Ca}_{0.3}\text{CoO}_3$. It is strange that spin-glass behavior is not found in $\text{Gd}_{0.55}\text{Sr}_{0.45}\text{Co}_{0.7}\text{Fe}_{0.3}\text{O}_3$ (see Fig.2 and Fig.3c) although T_c decreases by 30 K with Fe doping of 0.30 in $\text{Gd}_{0.55}\text{Sr}_{0.45}\text{CoO}_3$. This is in contrast to that observed in Fe-doped $\text{La}_{1-x}\text{Sr}_x\text{CoO}_3$ system, in which the strong spin-glass behavior is also found with the Fe doping level up to 0.30. [35, 36] Previous research [41] in $\text{Gd}_{1-y}\text{Sr}_y\text{CoO}_3$ have demonstrated that there is not spin-glass behavior at low Sr concentration, being in contrast to the spin-glass magnetism in $\text{La}_{1-x}\text{Sr}_x\text{CoO}_3$ ($x < 0.18$). The existence of Gd^{3+} ions with the *large magnetic moment* ($S = 7/2$) may be taken as one possible reason for the absence of spin-glass behavior in $\text{Gd}_{1-y}\text{Sr}_y\text{CoO}_3$ because the strong internal field produced by Gd^{3+} magnetic sublattice may reduce the relaxation time and destroy a spin-glass magnetism.

V. CONCLUSION

We systematically studied the effect of Fe doping on the magnetic and transport properties on the polycrystalline $\text{Pr}_{0.7}\text{Ca}_{0.3}\text{Co}_{1-x}\text{Fe}_x\text{O}_{3-\delta}$, $\text{Pr}_{0.55}\text{Ca}_{0.45}\text{Co}_{1-x}\text{Fe}_x\text{O}_{3-\delta}$ and $\text{Gd}_{0.55}\text{Sr}_{0.45}\text{Co}_{1-x}\text{Fe}_x\text{O}_3$. It is found that that Fe doping in $\text{Gd}_{0.55}\text{Sr}_{0.45}\text{CoO}_3$ strongly suppresses ferromagnetism, but does not induce spin-glass behavior; while Fe doping in $\text{Pr}_{1-y}\text{Ca}_y\text{CoO}_3$ enhances the ferromagnetism at low Fe doping level, but suppresses ferromagnetism and induced spin-glass magnetism in highly doped samples. Such contrasting response to Fe doping in $\text{Gd}_{0.55}\text{Sr}_{0.45}\text{CoO}_3$ and $\text{Pr}_{1-y}\text{Ca}_y\text{CoO}_3$ can be interpreted on the basis of the existences of the antiferromagnetic interactions through $\text{Fe}^{3+}\text{-O-Fe}^{3+}$ and $\text{Fe}^{3+}\text{-O-Co}^{3+}$ (IS) and ferromagnetic interactions through $\text{Fe}^{3+}\text{-O-Co}^{4+}$ (LS). In this picture, the average radius of the ions on A sites plays the key role in determining what type interaction Fe doping mainly introduces.

VI. ACKNOWLEDGEMENT

This work is supported by the Nature Science Foundation of China and by the Ministry of Science and Technology of China (973 project No: 2006CB601001), and by the Knowledge Innovation Project of Chinese Academy of Sciences.

* Electronic address: chenxh@ustc.edu.cn

-
- [1] See, for example, P. A. Lee, N. Nagaosa, and X. G. Wen, *Rev. Mod. Phys.* **78**, 17 (2006); D. N. Basov and T. Timusk, *Rev. Mod. Phys.* **77**, 721 (2005); E. Dagotto, *Rev. Mod. Phys.* **66**, 763 (1994); and references therein.
- [2] See the review, for example: M. B. Salamon and M. Jaime, *Rev. Mod. Phys.* **73**, 583 (2001); L. P. Gor'kov and V. Z. Kresin, *Phys. Rep.* **400**, 149 (2004); Y. Tokura, *Rep. Prog. Phys.* **69**, 797 (2006); and references therein.
- [3] R. Ramesh, B. Dutta, T. S. Ravi, J. Lee, T. Sands, and V. G. Keramidas, *Appl. Phys. Lett.* **64**, 1588 (1994).

- [4] M. K. Lee, T. K. Nath, C. B. Eom, M. C. Smoak, and F. Tsui, *Appl. Phys. Lett.* **77**, 3547 (2000).
- [5] N. Hur, S. Park, P. A. Sharma, J. S. Ahn, S. Guha and S. W. Cheong, *Nature* **429**, 392 (2004).
- [6] T. Kimura, S. Kawamoto, I. Yamada, M. Azuma, M. Takano, and Y. Tokura, *Phys. Rev. B* **67**, 180401 (2003).
- [7] A. Pimenov, A. A. Mukhin, V. Y. Ivanov, V. D. Travkin, A. M. Balbashov and A. Loidl, *Nature Phys.* **2**, 97 (2006).
- [8] M. Imada, A. Fujimori, and Y. Tokura, *Rev. Mod. Phys.* **70**, 1039 (1998).
- [9] W. C. Koehler and E. O. Wollan, *J. Phys. Chem. Solids* **2**, 100 (1957).
- [10] R. R. Heikes, R. C. Miller, and R. Mazelsky, *Physica (Amsterdam)* **30**, 1600 (1964).
- [11] G. Briceno, H. Y. Chang, X. D. Sun, P. G. Schultz, and X. D. Xiang, *Science* **270**, 273 (1995).
- [12] A. V. Samoilov, G. Beach, C. C. Fu, N.-C. Yeh, and R. P. Vasquez, *Phys. Rev. B* **57**, R14032 (1998).
- [13] S. A. Baily, M. B. Salamon, Y. Kobayashi, and K. Asai, *Appl. Phys. Lett.* **80**, 2138 (2002).
- [14] N. V. Kasper, I. O. Troyanchuk, D. D Khalyavin, N. Hamad, L. Haupt, P. Frobel, K. Barner, E. Gmelin, Q. Huang , and J. W. Lynn, *Physica Status Solidi B* **215**, 697 (1999).
- [15] Y. Moritomo, T. Akimoto, M. Takeo, A. Machida, E. Nishibori, M. Takata, M. Sakata, K. Ohoyama, and A. Nakamura, *Phys. Rev. B* **61**, R13325-R13328 (2000).
- [16] C. Frontera, J. L. Garcia-Munoz, A. Llobet, and M. A. G. Aranda, *Phys. Rev. B* **65**, 180405 (2002).
- [17] S. Tsubouchi, T. Kyômen, M. Itoh, P. Ganguly, M. Oguni, Y. Shimojo, Y. Morii, and Y. Yoshii, *Phys. Rev. B* **66**, 052418 (2002).
- [18] F. Faith, E. Suard, and V. Caignert, *Phys. Rev. B* **65**, 060401 (2001).
- [19] J. Wu, and C. Leighton, *Phys. Rev. B* **67**, 174408 (2003).
- [20] P. L. Kuhns, M. J. R. Hoch, W.G. Moulton, A. P. Reyes, J.Wu, and C. Leighton, *Phys. Rev. Lett.* **91**, 127202 (2003).
- [21] M. J. R. Hoch, P. L. Kuhns, W. G. Moulton, A. P. Reyes, J. Lu, J. Wu, and C. Leighton, *Phys. Rev. B* **70**, 174443 (2004).
- [22] A. Ghoshray, B. Bandyopadhyay, K. Ghoshray, V. Morchshakov, K. Bärner, I. O. Troyanchuk, H. Nakamura, T. Kohara, G. Y. Liu and G. H. Rao, *Phys. Rev. B* **69**, 064424 (2004).
- [23] N. N. Loshkareva, E. A. Gan'shina, B. I. Belevtsev, Y. P. Sukhorukov, E. V. Mostovshchikova,

- A. N. Vinogradov, V. B. Krasovitsky, and I. N. Chukanova, Phys. Rev. B **68**, 024413 (2003).
- [24] M. A. Korotin, S. Yu. Ezhov, I. V. Solovyey, V. I. Anisimov, D. I. Khomskii, and G. A. Sawatzky, Phys. Rev. B **54**, 5309 (1996).
- [25] S. Yamaguchi, Y. Okimoto, and Y. Tokura, Phys. Rev. B **55**, 8666 (1997).
- [26] D. Louca, J. L. Sarrao, J. D. Thompson, H. Roder, and G. H. Kwei, Phys. Rev. B **60**, R10 378 (1999).
- [27] Y. Kobayashi, N. Fujiwara, S. Murata, K. Asai, and H. Yasuoka, Phys. Rev. B **62**, 410 (2000).
- [28] C. Zobel, M. Kriener, D. Bruns, J. Baier, M. Gruninger, T. Lorenz, P. Reutler, and A. Revcolevschi, Phys. Rev. B **66**, 020402 (2002).
- [29] P. Ravindran, H. Fjellvag, A. Kjekshus, P. Blaha, K. Schwarz, and J. Luitz, J. Appl. Phys. **91**, 291 (2002).
- [30] K. Asai, O. Yokokura, M. Suzuki, T. Naka, T. Matsumoto, H. Takahashi, N. Mori, and K. Kohn, J. Phys. Soc. Jpn. **66**, 967 (1997); K. Asai, A. Yoneda, O. Yokokura, J. M. Tranquada, G. Shirane, and K. Kohn, *ibid.* **67**, 290 (1998).
- [31] R. Lengsdorf, M. Ait-Tahar, S. S. Saxena, M. Ellerby, D. I. Khomskii, H. Micklitz, T. Lorenz, and M. M. Abd-Elmeguid, Phys. Rev. B **69**, 140403 (2004).
- [32] T. Vogt, J. A. Hriljac, N. C. Hyatt, and P. Woodward, Phys. Rev. B **67**, 140401 (2003).
- [33] I. Fita, R. Szymczak, R. Puzniak, I. O. Troyanchuk, J. Fink-Finowicki, Ya. M. Mukovskii, V. N. Varyukhin, and H. Szymczak, Phys. Rev. B **71**, 214404 (2005).
- [34] A. Barman, M. Ghosh, S. Biswas, S.K. De, S. Chatterjee, Appl. Phys. Lett. **71**, 3150 (1997).
- [35] Y. Sun, X. J. Xu, and Y. H. Zhang, Phys. Rev. B **62**, 5289 (2000).
- [36] M. H. Phan, T. L. Phan, T. N. Huynh, S. C. Yu, and J. R. Rhee, J. Appl. Phys. **95**, 7531 (2004); T. L. Phan, S. C. Yu, N. V. Khiem, M. H. Phan, J. R. Rhee, and N. X. Phuc, J. Appl. Phys. **97**, 10A508 (2005);
- [37] Á. Cziráki, I. Geröcs, M. Köteles, A. Gábris, L. Pogány, I. Bakonyi, Z. Klencsár, A. Vértes, S. K. De, A. Barman, M. Ghosh, S. Biswas, S. Chatterjee, B. Arnold, H. D. Bauer, K. Wetzig, C. Ulhaq-Bouillet, and V. Pierron-Bohnes, Eur. Phys. J. B **21**, 521 (2001).
- [38] Z. Németh Z. Klencsár, E. Kuzmann, Z. Homonnay, A. Vértes, J.M. Grenéche, B. Lackner, K. Kellner, G. Gritzner, J. Hakl, K. Vad, S. Mészáros, and L. Kerekes, Eur. Phys. J. B **43**, 297 (2005)
- [39] X. G. Luo, X. Li, G. Y. Wang, G. Wu, and X. H. Chen, J. Solid State Chem. **179**, 2174 (2006)

- [40] S. Tsubouchi, T. Kyômen, and M. Itoh, Phys. Rev. B **69**, 144406 (2004).
- [41] X. G. Luo, H. Li, X. H. Chen, Y. M. Xiong, G. Y. Wang, C. H. Wang, W. J. Miao, and X. Li, Chem. Mater. **18**, 1029 (2006).
- [42] R. D. Shannon, Acta Crystallogr. **A32**, 751 (1976).
- [43] M. Kopcewicz, D. D. Khalyavin, I. O. Troyanchuk, H. Szymczak, R. Szymczak, D. J. Logvinovich, and E. N. Naumovich, J. Appl. Phys. **93**, 479 (2003).
- [44] Z. Homonnay, E. Kuzmann, Z. Nemeth, Z. Klencsar, S. I. Nagy, and A. Vertes, Ceramics-Silikaty **48**, 197 (2004).
- [45] K. Gunnarson, P. Svedlindh, P. Nordblad, L. Lundgren, H. Aruga, and A. Ito, Phys. Rev. Lett. **61**, 754 (1988).
- [46] J. A. Mydosh, *Spin-Glasses: An Experimental Introduction* (Taylor and Francis, London, 1993).
- [47] From Ref.[37], the ion radius of Gd^{3+} , Pr^{3+} , Ca^{2+} , La^{3+} and Sr^{2+} is 1.107, 1.179, 1.180, 1.216, and 1.310 Å, respectively.
- [48] S. Yamaguchi, Y. Okimoto, and Y. Tokura, Phys. Rev. B **54**, R11022 (1996).
- [49] J. B. Goodenough, Phys. Rev. B **100**, 564 (1955).
- [50] J. Kanamori, J. Chem. Phys. Solids **10**, 87 (1959).
- [51] J. B. Goodenough, *Magnetism and Chemical Bonds* (John Wiley & Sons, New York-London, 1963), pp. 174-178.

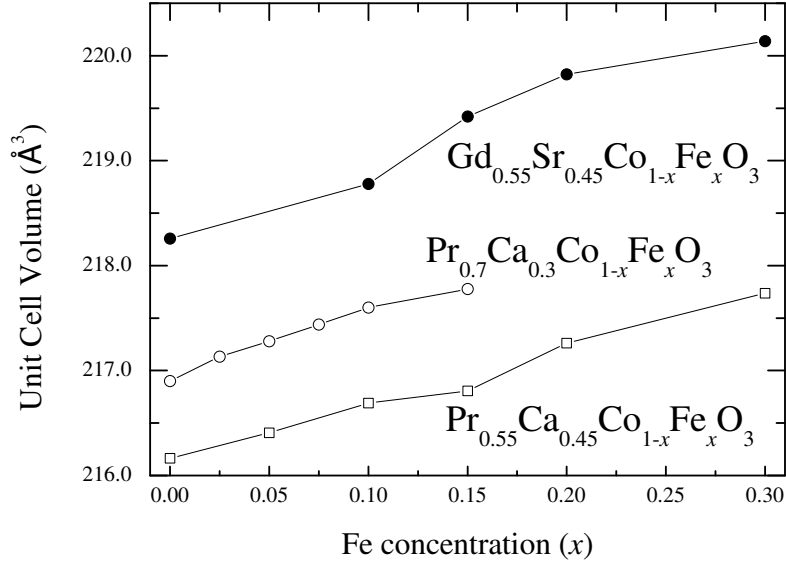


FIG. 1: Variation of unit cell volume with x for the polycrystalline $\text{Pr}_{1-y}\text{Ca}_y\text{Co}_{1-x}\text{Fe}_x\text{O}_3$, and $\text{Gd}_{0.55}\text{Sr}_{0.45}\text{Co}_{1-x}\text{Fe}_x\text{O}_3$.

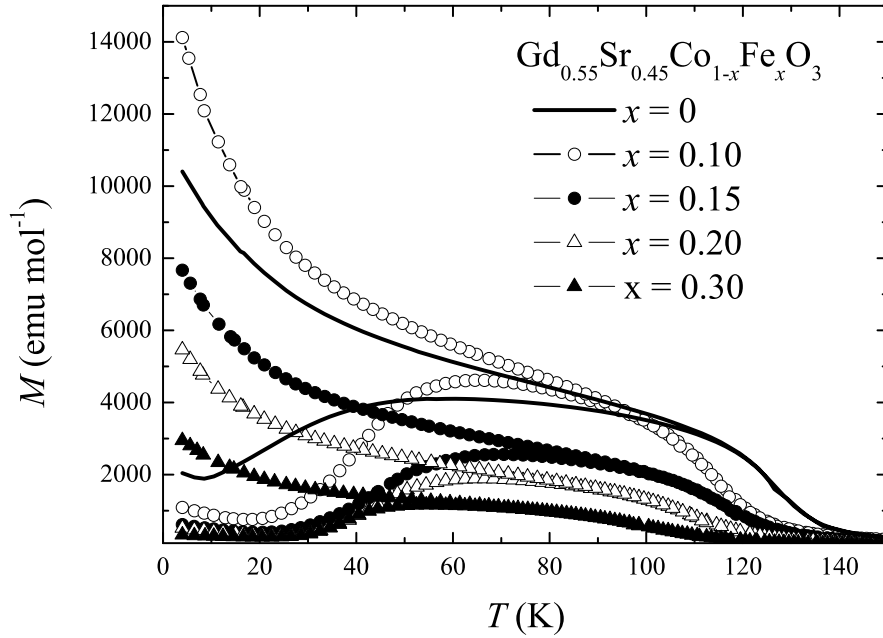


FIG. 2: Temperature dependence of the molar magnetization recorded at $H = 0.1$ T for the polycrystalline samples $\text{Gd}_{0.55}\text{Sr}_{0.45}\text{Co}_{1-x}\text{Fe}_x\text{O}_3$.

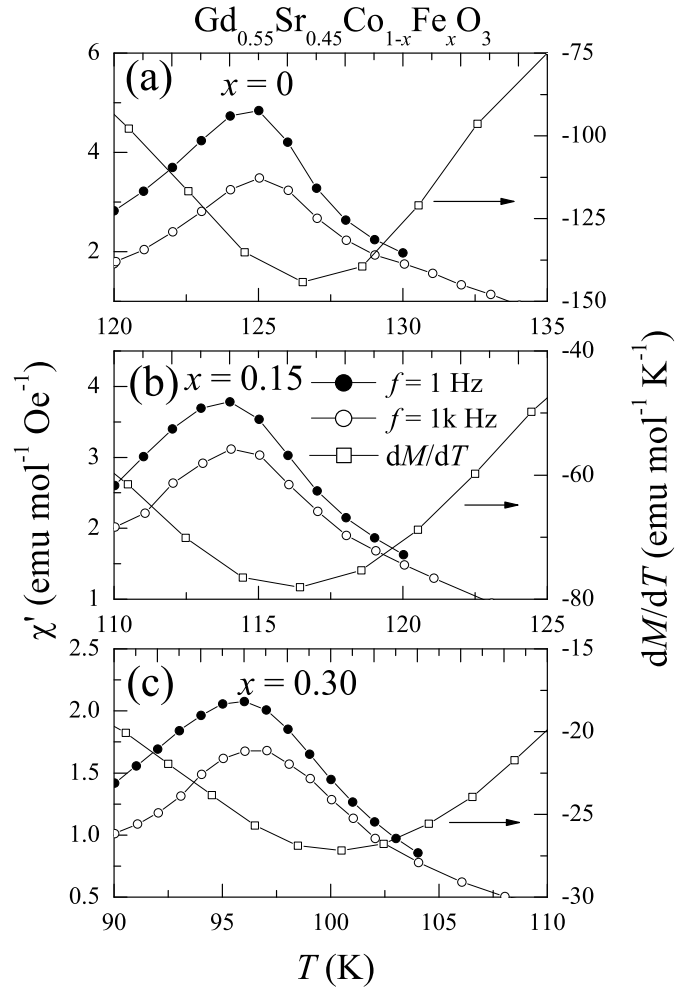


FIG. 3: Temperature dependence of in-phase ac susceptibility $\chi'(T)$ at 1 Hz and 1 kHz measured in ac the magnetic field of 3.8 Oe for $\text{Gd}_{0.55}\text{Sr}_{0.45}\text{Co}_{1-x}\text{Fe}_x\text{O}_3$ with $x = 0, 0.1,$ and 0.3 . As a comparison to dc data, the dM/dT is plotted together with the ac data.

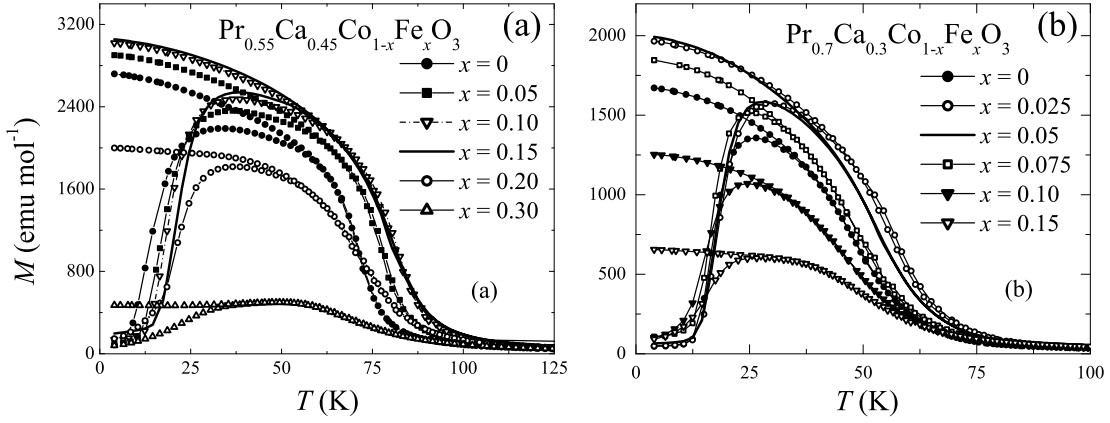


FIG. 4: Temperature dependence of the molar magnetization recorded at $H = 0.1$ T for the polycrystalline samples: (a) $\text{Pr}_{0.55}\text{Ca}_{0.45}\text{Co}_{1-x}\text{Fe}_x\text{O}_3$ and (b) $\text{Pr}_{0.7}\text{Ca}_{0.3}\text{Co}_{1-x}\text{Fe}_x\text{O}_3$.

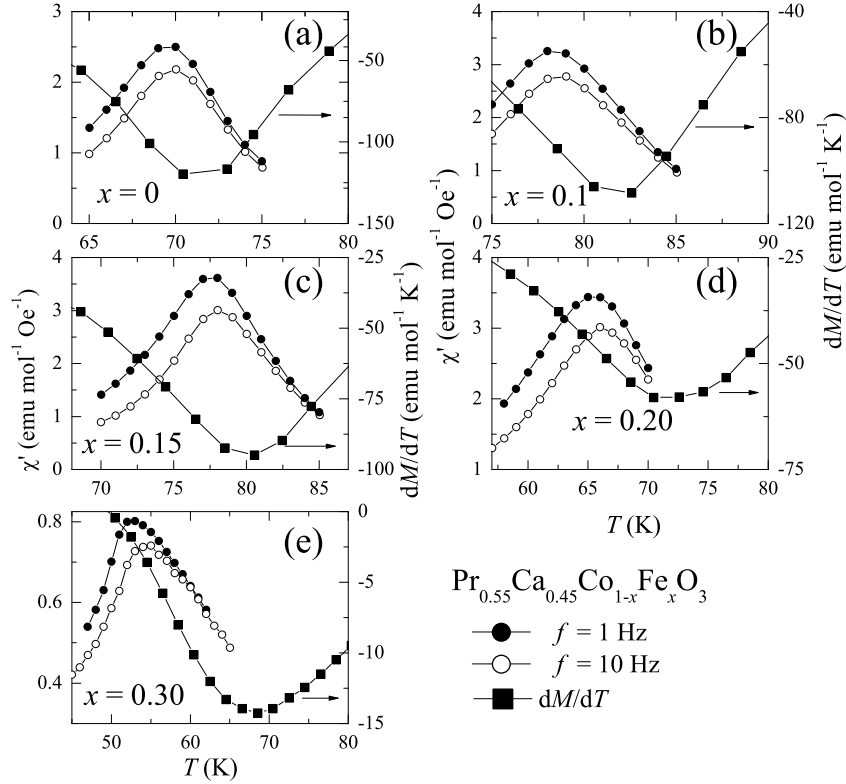


FIG. 5: Temperature dependence of in-phase ac susceptibility $\chi'(T)$ at 1 Hz and 1 kHz measured in ac the magnetic field of 3.8 Oe for $\text{Pr}_{0.55}\text{Ca}_{0.45}\text{Co}_{1-x}\text{Fe}_x\text{O}_3$ with $x = 0, 0.1, 0.15, 0.2, \text{ and } 0.3$. As a comparison to dc data, the dM/dT is plotted together with the ac data.

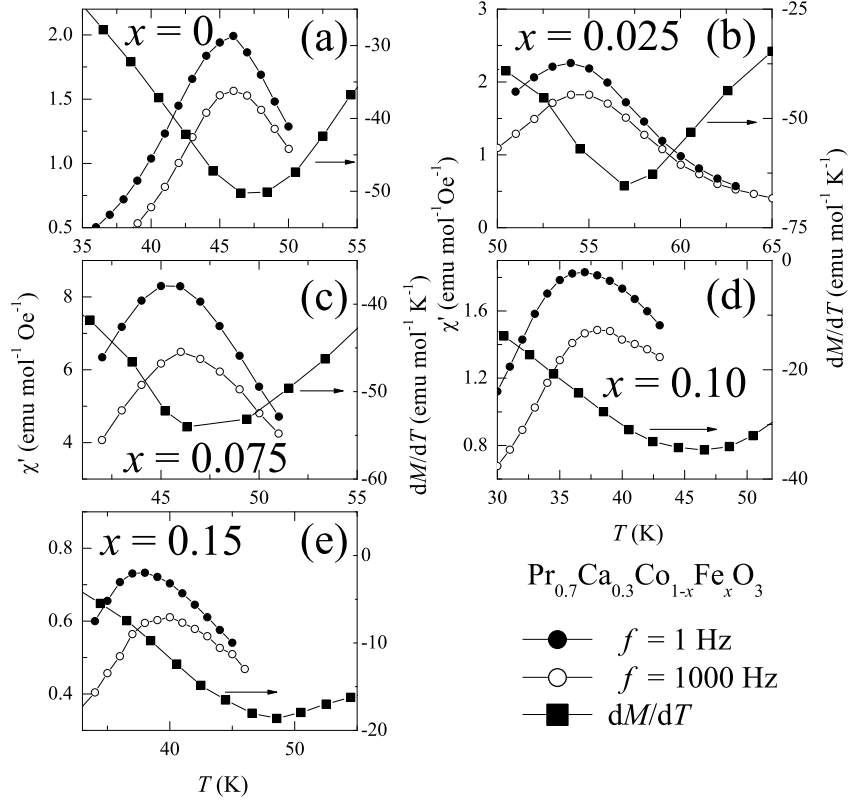


FIG. 6: Temperature dependence of in-phase ac susceptibility $\chi'(T)$ at 1 Hz and 1 kHz measured in ac the magnetic field of 3.8 Oe for $\text{Pr}_{0.7}\text{Ca}_{0.3}\text{Co}_{1-x}\text{Fe}_x\text{O}_3$ with $x = 0, 0.025, 0.075, 0.1, \text{ and } 0.15$. As a comparison to dc data, the dM/dT is plotted together with the ac data.

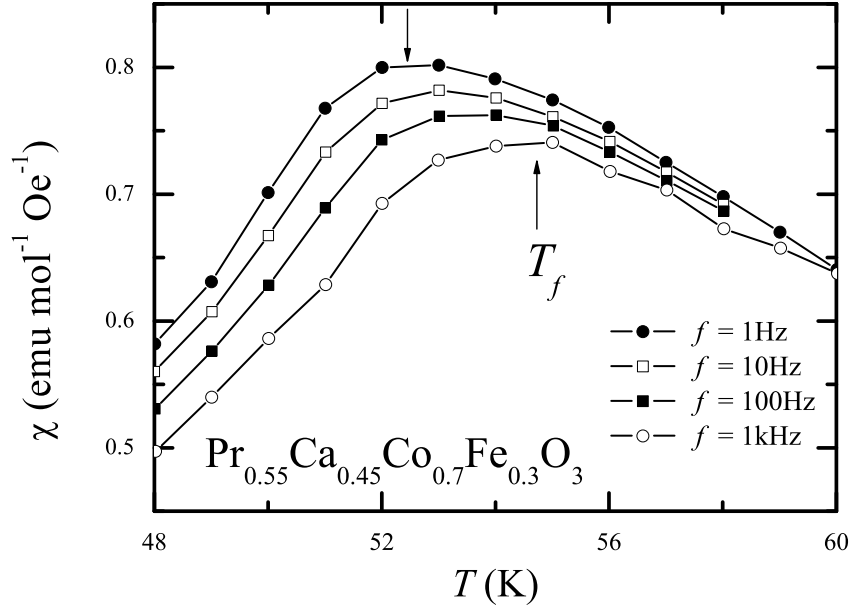


FIG. 7: Closeup of the temperature dependence of the in-phase ac susceptibility for $\text{Pr}_{0.55}\text{Ca}_{0.45}\text{Co}_{0.7}\text{Fe}_{0.3}\text{O}_3$, at four different frequencies in the range 1 – 1000 Hz.

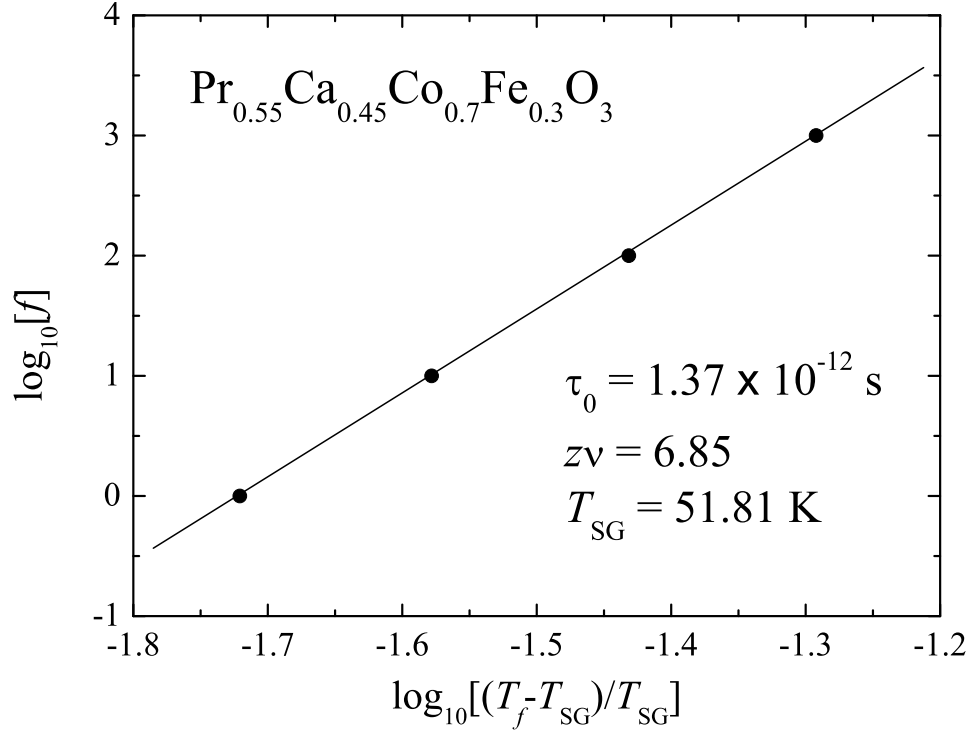


FIG. 8: $\log_{10}[f]$ vs $\log_{10}[(T_f - T_{SG})/T_{SG}]$ for $\text{Pr}_{0.55}\text{Ca}_{0.45}\text{Co}_{0.7}\text{Fe}_{0.3}\text{O}_3$, demonstrating good agreement with Eq. (1). T_f is determined by the temperature with $d\chi'(T)/dT = 0$. The solid line is a best fit to the data with the parameters shown in the figure.

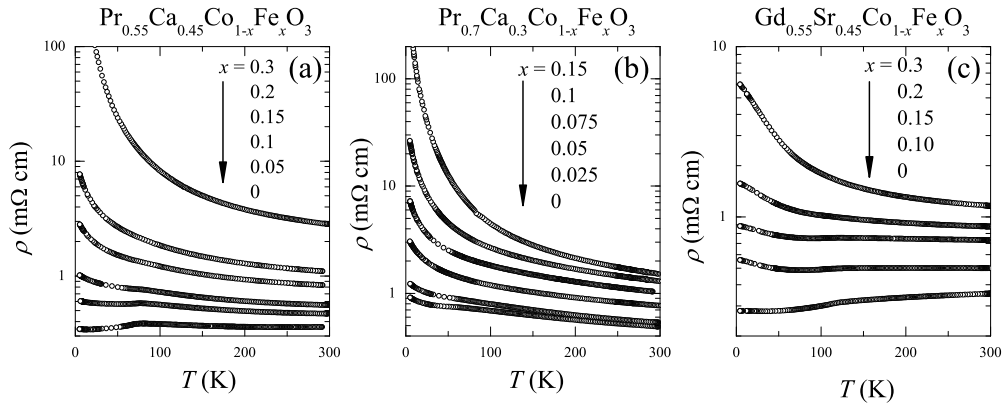


FIG. 9: Temperature dependence of resistivity for the polycrystalline samples of: (a) $\text{Pr}_{0.55}\text{Ca}_{0.45}\text{Co}_{1-x}\text{Fe}_x\text{O}_3$; (b) $\text{Pr}_{0.7}\text{Ca}_{0.3}\text{Co}_{1-x}\text{Fe}_x\text{O}_3$; (c) $\text{Gd}_{0.55}\text{Sr}_{0.45}\text{Co}_{1-x}\text{Fe}_x\text{O}_3$.

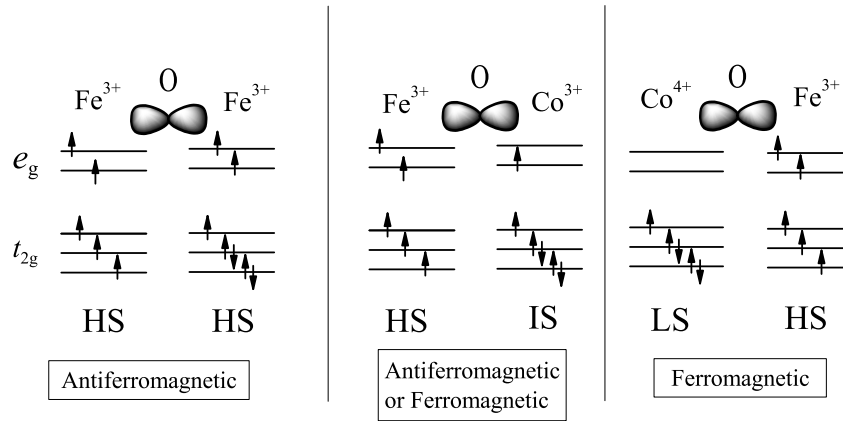


FIG. 10: Schematic model for the spin state configuration of Fe^{3+} , Co^{4+} and of Fe^{3+} , Co^{3+} (left and right, respectively). The oxygen orbitals are also drawn. HS, IS, and LS represent high, intermediate and low spin, respectively.